Accepted Manuscript

Finite-size effects in simulations of self-propelled particles system

Dorilson. S. Cambui, M. Godoy, A.S. de Arruda

PII: S0378-4371(16)30728-2
DOI: http://dx.doi.org/10.1016/j.physa.2016.10.041
Reference: PHYSA 17599

To appear in: *Physica A*

Received date: 1 June 2016
Revised date: 28 August 2016

Please cite this article as: D.S. Cambui, M. Godoy, A.S. de Arruda, Finite-size effects in simulations of self-propelled particles system, *Physica A* (2016), http://dx.doi.org/10.1016/j.physa.2016.10.041

HIGHLIGHTS:

- We model self-propelled particles system used to study the live organisms motion;
- Important parameters in this system are velocity, interaction radius and density;
- We estimate a set of critical exponents as function of these parameters;
- We find that such parameters, in turn, influences the values of critical exponents;
- Critical exponents obtained satisfy the hyperscaling relationship.

Finite-size effects in simulations of self-propelled particles system

Dorilson. S. Cambui[a,b,*], M. Godoy[c], A. S. de Arruda[c]

[a] *Secretaria de Estado de Educação de Mato Grosso, 78049-909, Cuiabá, Mato Grosso, Brazil*
[b] *Universidade do Estado de Mato Grosso, UNEMAT, Departamento de Matemática, Barra do Bugres, Mato Grosso, Brazil*
[c] *Instituto de Física, Universidade Federal de Mato Grosso, 78060-900, Cuiabá, MT, Brazil*

Abstract

We have considered a generalized version of a model consisting of self-propelled particles, where the speed is treated as a independent stochastic variable described by a Gamma-distribution, and the motion direction is adjusted in according to two behavioral rules: repulsion and orientation. We used the finite-size scaling theory to estimate the static critical exponents β, γ and ν as a function of the density ρ. We have obtained different values of the critical exponents for different values of the density ρ.

1. Introduction

The interest in understanding the collective behavior of living systems [1, 2, 3] provides a fertile ground of novel models and studies in statistical physics. In this aspect in last years has grown interest in understanding such collective behavior [4, 5], which seem to be quite robust and universal. The collective behavior is a fascinating feature that can be displayed in several systems and on many different scales. As examples observed in nature include mammal herds[6], fish schools [7], bird flocks [8], crowds of pedestrians [9, 10], insect swarms [11, 12, 13], bacterial colonies [14, 15, 16, 17] and molecular motors [18, 19]. Certainly, biological groups must have some advantages in

*Corresponding author
Email address: dcambui@fisica.ufmt.br (Dorilson. S. Cambui)

to present this collective behavior, i.e., the ability to align and itself move around in a same direction. Such advantages can be the increasing the chance of finding food, avoid predators [20] and increase in the reproduction rate and forage [21].

On the other hand, the concept of self-propelled particles was employed to describe the collective motion of groups of autonomous agents, therefore, in this context Vicsek *et al.* [22, 23] proposed a minimal model of self-propelled particles to mimic the dynamics of biological swarms. This model was defined on a continuous plane which has the point particles, with a constant velocity, representing such agents. Then the particles, at each time step, adopt the average motion direction of its neighboring within an interaction range r_o, centered at the current position of the particle i, with a constant velocity of modulus ν_0. In nature there is no perfect motion, thus random perturbations are added in the individual moving direction. Such perturbations are called of noise and are used for represents measurement errors in detection of the movement direction of the nearest neighbors. Vicsek *et al.* shown that this model displayed the presence of a non-equilibrium phase transition from a disordered state, at high enough noise, to a state with collective motion, which it was classified as a second-order phase transition. The occurrence of a order-disorder phase transition in biological systems was observed in marching locusts [25]. Similar results were also obtained (by increasing the density of Tilapia fish) in fish schools[26], and in collective migration of cells [27]. Another transition from a disordered, where no global order is found, to an ordered phase has been observed in large population of spawning herrings by Makris *et al.* [28].

In the original formulation of the Vicsek model, the only interaction rule is the directional alignment, unlike other models that incorporate behavioral rules such as repulsion, alignment and attraction into their simulations [24, 29, 30, 31]. In general, a variety of research have been used to model and explore the dynamic properties of self-propelled particles [32, 33, 34, 35, 36, 37, 38, 39, 40, 41, 42, 43, 44].

In nature, many animal groups display coordinated motion in which individuals too close to one another will repel themselves, in order to avoid collision and plus the tendency to align their motion direction with nearest neighbors. In this context, we consider a generalized version for self-propelled particles which follows biologically motivated behavioral rules, where the interactions are limited to attraction and alignment and the speed is treated as an independent stochastic variable. These behavioral interactions occur

within two regions: orientation zone and repulsion zone. For the specific case in which no neighbors are "to be seen" in the repulsion zone, the model reduces to Vicsek model. The particles that access these interaction zones have their motion directions updated with a random noise added. In the repulsion zone, of radius r_r, the motion direction of each particle is generated by repulsive interactions with the other neighbors individuals. In orientation zone, of radius r_o, the update of the velocity direction follows here the same rule used in the original Vicsek model. In addition, as in nature different agents may have different speeds, here each particle has a speed independent of the others. Therefore, It is determined by a Gamma distribution, which it is a distribution observed in biological groups as described in the references [30, 45].

In our previous work [4], we calculated the critical exponents (β, γ and ν) of a self-propelled particle system, but using the original formulation of the Vicsek model. Based on a greater biological realism (speed independent and repulsive interactions), our aim in this paper is to estimate the static critical exponents of the model. We employed finite-size scaling arguments to estimate the values of static critical exponents β (order parameter critical exponent), ν (correlation-length critical exponent) and γ (susceptibility critical exponent) at the critical point of the system.

The rest of this paper is organized as follows: The detailed formulation of the model and the simulation parameters are presented in Section 2. A brief description of the finite-size scaling theory is discussed in Section 3. We present the results of our simulations in Section 4 and the main conclusions are presented in Section 5.

2. The model and simulation parameters

We have performed the simulations in two dimensions where the organisms are represented by N particles moving on a $L \times L$ square lattice, with periodic boundary conditions, in which the density is given by $\rho = N/L^2$. The positions and directions are initially randomly distributed. Aiming greater biological realism, this model is composed of two interactions regions called of repulsion zone (REP) of radius r_r and orientation zone (ORI) of radius r_o with N_r and N_o neighbors particles j respectively, see Fig. 1.

Every individual i has access to these zones according to the distance d_{ij} between them. The position $\mathbf{x}_i(t)$ and the velocity $\mathbf{v}_i(t)$ vectors are updated

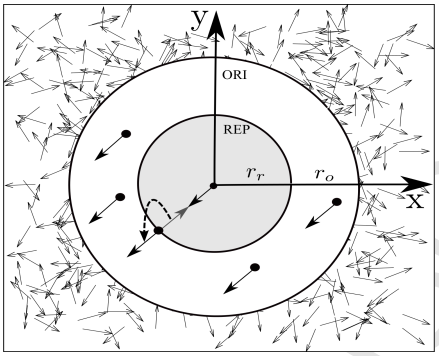

Figure 1: Schematic representation of the behavioral zones. In the repulsion zone (represented by the inner circle with radius r_r, REP) individuals apart from each other and in the orientation zone (outer circle with radius r_o, ORI) align themselves with a same speed. In external region we have a random initial configuration of the movements simulated in time $t = 0$.

simultaneously according to,

$$\mathbf{x}_i(t + \Delta t) = \mathbf{x}_i(t) + \mathbf{v}_i(t)\Delta t. \tag{1}$$

The magnitude of the velocity of the particles is fixed to v. The speed v_i, of each particles i ($i = 1,...,N$), is determined independently of others. This speed is a stochastic variable characterized by a probability distribution, however, here it is described by a Gamma distribution, whose probability density function is

$$F(v) = \frac{a^k}{\Gamma(k)} e^{-av} v^{k-1}, \tag{2}$$

where $\Gamma(k)$ is Gamma function, a is a positive constant called scale parameter and k is a positive integer constant known as the shape parameter. We choose their values based in previous observations by Aoki [45], in which $k = 4$ and $a = 3.3$. X is a random variable uniformly distributed among $[0, 1]$.

In the interactions regions, each individual adjust its motion direction according to the behaviors of repulsion and orientation of its neighbors, and also adjust its speed (of interaction) v_{int}, which becomes equal to the average value of the speeds of all agents,

$$v_{int} = \frac{1}{N} \sum_{i=1}^{N} v_i, \tag{3}$$

In the repulsion zone, of radius r_r, the individual maintain a minimum distance from its nearest neighbors to avoid collisions, turning in the opposite direction. Such as used in [31], the updating of the motion direction in this zone is

$$\mathbf{d}_i^{(REP)} = -\sum_{j\neq i}^{N_r} \mathbf{r}_{ij} \Big/ \mid \sum_{j\neq i}^{N_r} \mathbf{r}_{ij} \mid, \tag{4}$$

where $\mathbf{r}_{ij}$ is the unit vector pointing from the individual i in the direction from the j-th neighbor ($j = 1, \ldots, N_r$) and $\mathbf{r}_{ij} = (\mathbf{r}_j - \mathbf{r}_i)/ \mid \mathbf{r}_j - \mathbf{r}_i \mid$.

If the repulsion zone contains no neighbors, the individual i will respond to neighbors within the orientation zone for align to motion of other particles. The motion direction, including i, is given by average of the velocities of all its N_o neighbors, such that

$$\mathbf{d}_i^{(ORI)} = \sum_{j=1}^{N_o} \mathbf{v}_j \Big/ \mid \sum_{j=1}^{N_o} \mathbf{v}_j \mid. \tag{5}$$

Due the uncertainty that the particle i has of the position of its neighbors, the motion direction is perturbed by a random noise $\xi\eta$, where ξ is a random variable chosen with an uniform probability on the interval $[-\pi, \pi]$ and η is the amplitude of the noise. The order parameter adopted here is one originally defined by Vicsek *et al.* [22], as the absolute value of the normalized mean velocity.

Here, we have proposed a version for self-propelled particles in which different agents have different speeds v_i obtained of the Gamma distribution. During the simulation time, the individual adjust its motion direction according to the behaviors of repulsion and orientation of its neighbors and also its speed, which must be equal to the limit defined by Eq. (3). We performed numerical simulations for various lattice sizes and fixed values of the number of particles $N = 100$, 200, 300, 500 and 1000. We have adopted periodic boundary conditions.

The results presented in this paper were obtained through of a number of independent runs with discrete time step $\Delta t = 1$. We defined the repulsion radius (set as $r_r = 1$), so as to maintain a private zone. The orientation radius, where individuals tend to align their motion, was set as $r_o = 2$.

In order to find the critical exponents as a function of the density, we have considered the following densities: $\rho = 0.05$, 0.1, 0.4, 1, 2, 3, 4, 5 and 6.

For each ρ the lattice size is $L = \sqrt{(N/\rho)}$. All our data was obtained over 8×10^5 time step to estimate the average values of the quantities of interest. In order to reach the equilibrium state, we have discarded the firsts 1×10^5 time step.

3. Finite-size scaling analysis

Finite-size scaling analysis is a very useful technique in order to find the correct values of the critical exponents of the system. In this work, we have employed finite-size scaling arguments [46, 47] to estimate the values of the static critical exponents β, ν and γ, at the critical point of the system. β is the order parameter, ν is the correlation length and γ is the susceptibility critical exponent. The order parameter, which measures the degree of alignment of the velocities, is defined by

$$\psi = \left| \frac{\sum_{i=1}^{N} \mathbf{v}_i(t)}{\sum_{i=1}^{N} \mid \mathbf{v}_i \mid} \right|. \tag{6}$$

The shape of the curve of ψ (see Fig. 2(a)) suggests, as pointed out in reference [22], the presence of a second-order phase transition in the system.

The susceptibility χ, that presents a peak around the critical noise for finite systems, is given by

$$\chi = L^2 \left(\langle \psi^2 \rangle - \langle \psi \rangle^2 \right), \tag{7}$$

where $\left(\langle \psi^2 \rangle - \langle \psi \rangle^2 \right)$ is the variance of the order parameter.

We have used the fourth-order Binder cumulant [46] to characterize the nature of the phase transition and to determine the critical exponent ν, and can be written by

$$C = 1 - \frac{\langle \psi^4 \rangle}{3 \langle \psi^2 \rangle^2}. \tag{8}$$

Our model for self-propelled particles exhibits a second-order phase transition between a collective ordered state of motion and a disordered regime. This can be easily observed by the behavior of the thermodynamic quantities present in Fig. 2. We also can observe the finite-size effects of the order parameter ψ_L (Fig. 2(a)), of the fourth-order Binder cumulant C_L (Fig. 2(b)) and of the susceptibility χ_L (Fig. 2(c)) as a function of noise η, and for

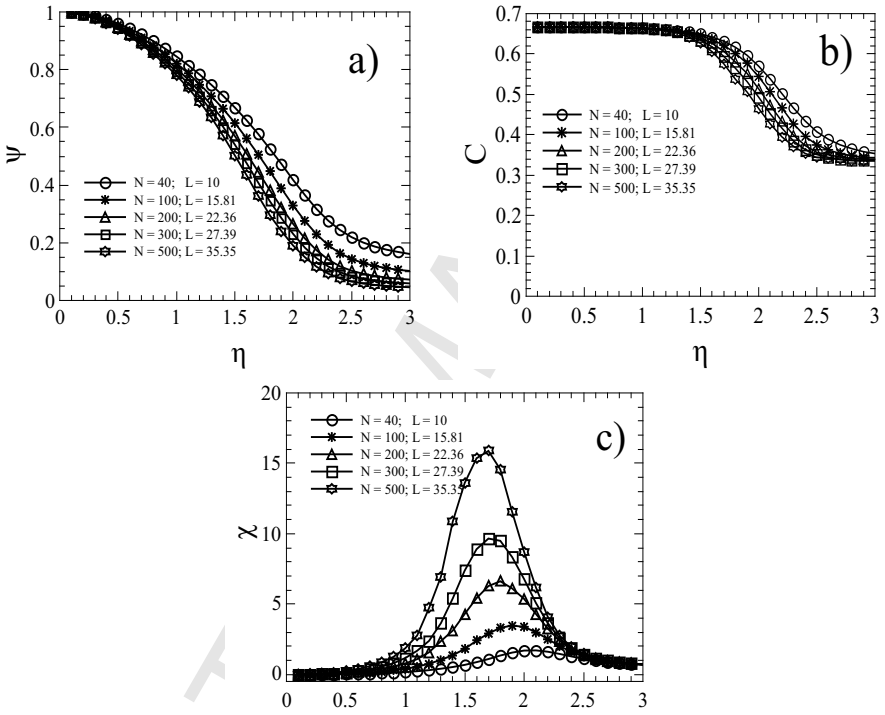

Figure 2: Finite-size behavior for various lattice size L, as indicated in the figures. (a) Order parameter $\psi_L(\eta)$, (b) fourth-order Binder cumulant $C_L(\eta)$ and (c) susceptibility $\chi_L(\eta)$ as a function of the noise η. All data are for a density $\rho = 0.4$. The error bars are smaller than the size of the symbols, and the lines serve as a guide to the eyes.

various system sizes L. We can see in Fig. 2(a) that the order parameter ψ_L vanishes with the increase of the noise η, indicating indeed the existence of a phase transition. The Binder cumulant C_L as a function of the noise η has a smooth behavior, indicating a second-order phase transition, but the value decreases significantly at the transition point, see Fig. 2(b). The susceptibility χ_L as a function of the noise η is shown in Fig. 2(c). For finite systems χ_L presents a peak around the critical noise η_c, which grows in height with the increase of the system size.

Around the critical noise η_c, we can evaluate the critical exponents associated with this transition, employing finite-size scaling relations [46, 47, 48] for the quantities defined by Eqs. (6), (7) and (8), that can be written as,

$$\psi_L = L^{-\beta/\nu}\psi_{\pm}(L^{1/\nu}\varepsilon), \tag{9}$$

$$\chi_L = L^{\gamma/\nu}\chi_{\pm}(L^{1/\nu}\varepsilon), \tag{10}$$

$$C_L = C_{\pm}(L^{1/\nu}\varepsilon), \tag{11}$$

where $\varepsilon = (\eta - \eta_c)/\eta_c$, $\psi_{\pm}$, $\chi_{\pm}$ and $C_{\pm}$ are scaling functions and $+$ or $-$ index refers to $\eta > \eta_c$ and $\eta < \eta_c$ respectively.

In order to estimate the critical exponent ν, we have used the derivative of Eq. (11) with respect to the noise η and that give us the following scaling relation:

$$C'_L(\eta) = L^{1/\nu}\frac{C'_{\pm}(L^{1/\nu}\varepsilon)}{\eta_c}. \tag{12}$$

Therefore with a log-log plot of $C'_L(\eta_c)$ versus L, we found the critical exponent ν from the slope of the straight line.

Finally, at the critical point, the relations (9), (10) and (12) yield,

$$\psi_L(\eta_c) = L^{-\beta/\nu}\psi_{\pm}(0), \tag{13}$$

$$\chi_L(\eta_c) = L^{\gamma/\nu}\chi_{\pm}(0), \tag{14}$$

$$C'_L(\eta_c) = L^{1/\nu}\frac{C'_{\pm}(0)}{\eta_c}. \tag{15}$$

We estimate the critical noise, through the location the maximum of the susceptibility [48] χ_{max}, whose peaks can be taken as a pseudocritical noise $\eta_{max}(L)$ which approaches η_c when $L \to \infty$.

4. Result for the critical exponents

Figs. 3(a), (b) and (c) display log-log plots of ψ_L, χ_L and C'_L, respectively, as a function of the linear size L at the critical point. The error bar for each point is included in these plots. At the critical point, log-log plots of $C'_L(\eta_c)$, $\psi_L(\eta_c)$ and $\chi_L(\eta_c)$ versus L must be a straight line with slopes $1/\nu$, β/ν and γ/ν, respectively. The best fit found to the data points gives us corresponding critical exponents.

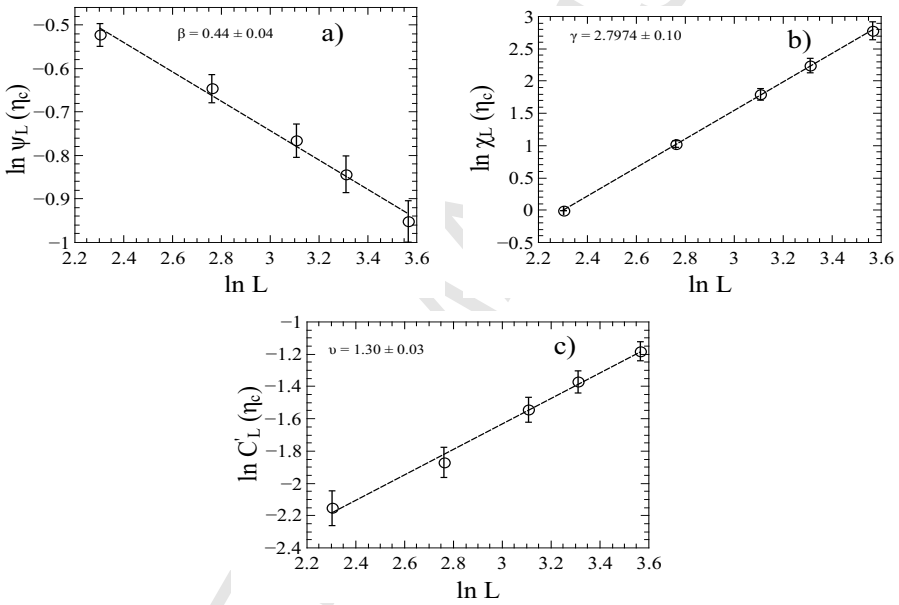

Figure 3: Log-log plots of (a) $\psi_L(\eta_c)$, (b) $\chi_L(\eta_c)$ and (c) $C'_L(\eta_c)$ as a function of the lattice size L, at the critical point, for $\rho = 0.4$. The straight lines are best fits to the data points. The results from the slopes are presented in figures and in Tab. (1).

Vicsek *et al.* [22] calculated the critical exponent associated with the order parameter, for a given density $\rho = 0.4$ and a velocity $v_0 = 0.03$, and they found $\beta = 0.45 \pm 0.07$. From the best fit to the data points, we have found $\beta = 0.44 \pm 0.04$ (Fig. 3(a)), $\gamma = 2.74 \pm 0.10$ (Fig. 3(b)) and $\nu = 1.30 \pm 0.03$ (Fig. 3(c)), for $\rho = 0.4$. The value that we found for β is according to the obtained by Vicsek (within the margin of error). However, the work of Vicsek did not indicate the calculation of the exponents ν and γ.

To obtain a more precise value of the critical exponents β and ν, we used the full data collapse of $\psi_L L^{\beta/\nu}$ versus $\varepsilon L^{1/\nu}$. For instance, we exhibit

in Figs. 4(a) and (b) the data collapses. From the slopes of these curves we have determined the critical exponents β and ν, and we can compare it with result obtained by slopes of the Figs. 3(a) and (c). The straight lines represent the asymptotic behavior of the scaling functions. The data points for all the values considered of N and L for a density $\rho = 0.4$ are located on two different branches: one upper branch ($\varepsilon < 0$) which characterizes the directional disorder phase and the one lower branch ($\varepsilon > 0$) related to the ordered phase. In Fig. 4(a), the best data collapse of the data points was found employing the exponent $\beta = 0.45$ obtained for Vicsek, in this case the best estimates give us $\nu = 1.3$. On the other hand, in Fig. 4(b) we used $\beta = 0.44$ and found $\nu = 1.3$. In both Figures, for $\varepsilon < 0$ we determine the exponents β and for $\varepsilon > 0$ the slopes of these curves give $\beta - \nu$.

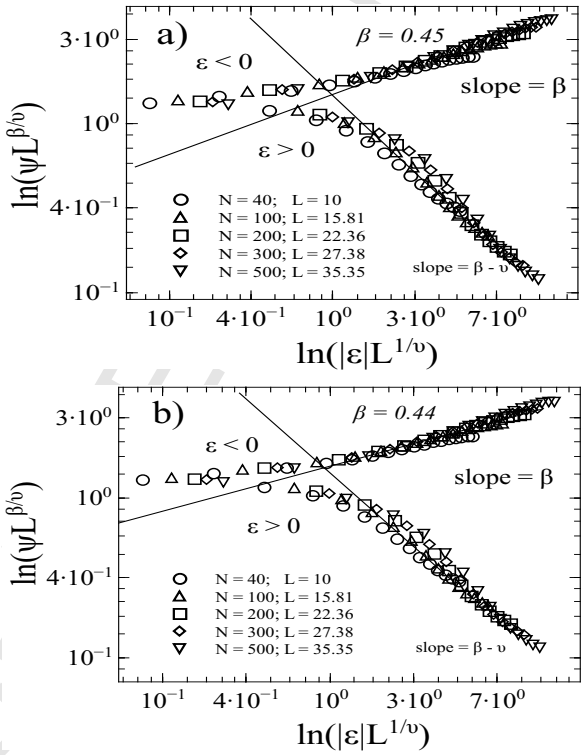

Figure 4: Finite-size scaling (full data collapse) near the critical point for the order parameter ψ_L, and for different values of N and L, as indicated in the figures. The parameter ε is defined by $\varepsilon = (\eta - \eta_c)/\eta_c$. The straight lines represent the asymptotic behavior of the scaling functions. (a) We have used $\beta = 0.45$ (by Vicsek) and found $\nu = 1.3$. (b) We found $\beta = 0.44$ and $\nu = 1.3$.

Finite-size effects of the order parameter ψ_L also were studied for other densities, such as: $\rho = 0.05$, 0.1, 0.4, 1, 2, 3, 4, 5 and 6. In Fig. 5, we display the results from the the straight line slopes of log-log plots for ψ_L, χ_L and C'_L as function of the density ρ. We have maintained the particles number according to $N = 40$, 100, 200, 300 and 500 and varied the lattice size L for each density mentioned above. At the critical point, log-log plots of $C'_L(\eta_c)$, $\psi_L(\eta_c)$ and $\chi_L(\eta_c)$ versus lattice size L must be a straight line with slopes $1/\nu$, β/ν and γ/ν, respectively. The best fit found to the data points furnishes us corresponding critical exponents. We can observe in Fig. 5 that the values of ν and γ decrease with increased of ρ, and β is almost constant. We also summarized in Tab. (1) the values of critical exponents as well as the respective critical noise.

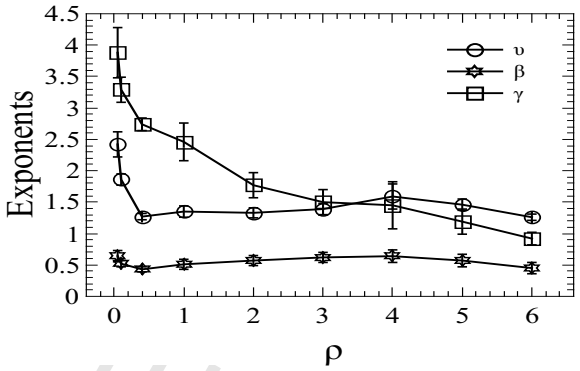

Figure 5: Critical exponents ν, β and γ as a function of the density ρ. The values were obtained from the straight line slopes of log-log plots for $C'_L(\eta_c)$, $\psi_L(\eta_c)$ and $\chi_L(\eta_c)$. The results also are presented in Tab. (1). The lines serve as a guide to the eyes.

ρ	η_c	ν	β	γ
0.05	0.60	2.42 ± 0.20	0.64 ± 0.03	3.88 ± 0.40
0.1	0.84	1.86 ± 0.09	0.52 ± 0.03	3.29 ± 0.20
0.4	1.67	1.27 ± 0.05	0.43 ± 0.04	2.74 ± 0.10
1.0	2.41	1.35 ± 0.09	0.51 ± 0.08	2.46 ± 0.30
2.0	2.88	1.33 ± 0.08	0.57 ± 0.08	1.77 ± 0.20
3.0	3.00	1.39 ± 0.09	0.62 ± 0.08	1.51 ± 0.20
4.0	3.21	1.59 ± 0.20	0.64 ± 0.10	1.45 ± 0.40
5.0	3.30	1.46 ± 0.09	0.57 ± 0.10	1.19 ± 0.20
6.0	3.36	1.26 ± 0.05	0.45 ± 0.09	0.92 ± 0.10

Table 1: Critical noise η_c and critical exponents ν, β and γ, for different values of the density ρ. All data were obtained by using the following parameters: $r = 1$ and $v_0 = 0.03$.

5. Conclusions

We have considered another version of the Vicsek model, based on local individual behavior rules in that was considered a repulsion zone in order to preserve, for biological reasons, the physical integrity of individuals that attempt, at all time, to maintain a minimum distance each others. In addition, to include some biological realism, the speed distribution incorporated as stochastic variable is described by a Gamma distribution. We have verified that the model exhibits a continuous phase transition which was indeed expected, since a second-order transition between an ordered state and a disordered regime was found in the Vicsek model. By employing finite-size scaling arguments from the equilibrium phase transitions theory, we have studied the influence of the density of particles on critical behavior of the system. We determined the static critical exponents of the model for a wide reach of density. Our results indicate that the parameter ρ influences the values of the critical exponents. A similar result was found by Tarras *et al.* [49] that proposed a Vicsek-type model, where they added a repulsion zone in order to avoid collisions between the particles. They calculated the critical exponents (using another method) for different repulsion radiuses and densities, and showed that exponents depend greatly on the size of these parameters indicating the non-universality of these critical exponents (depend on the details of the model).

Acknowledgments

Financial support from the Brazilian Agencies CNPq, CAPES (002/2012) and FAPEMAT (Grant No. 685524/2010) is gratefully acknowledged.

References

References

[1] J. Toner, Y. Tu, S. Ramaswamy, Annals of Physics 318 (2005) 170.

[2] L. Zhixin, G. Lei, Automatica 45 (2009) 2744.

[3] E. Ben-Jacob, I. Cohen, H. Levine, Advances in Physics 49 (2000) 395.

[4] D. Cambui, A. S. de Arruda, M. Godoy, Physica A 444 (2015) 582.

[5] E. Bertin, M. Droz, G. Grégoire, Journal of Physics A-mathematical and Theoretical 42 (2009) 445001.

[6] J. K. Parrish, W. M. Hamner, Animal Groups in Three Dimensions (Cambridge: Cambridge University Press) (1997).

[7] S. Hubbard, P. Babak, S.T. Sigurdsson, K.G. Magnusson, Ecological Modelling 174 (2004) 359.

[8] C. W. Reynolds, Computer Graphics 21 (1987) 25.

[9] D. Helbing, I. Farkas, T. Vicsek, Nature 407 (2000) 487.

[10] D. Helbing, I.J. Farkas, T. Vicsek, Physical review letters 84 (2000) 1240.

[11] E.M. Rauch, M.M. Millonas, D.R. Chialvo, Physics Letters A 207 (1995) 185.

[12] E. Bonabeau, G. Theraulaz, V. Fourcassi, J.-L. Deneubourg, Physical Review E 57 (1998) 4568.

[13] A.-C. Mailleux, J.-L. Deneubourg, C. Detrain, Animal behaviour 59 (2000) 1061.

[14] E. Ben-Jacob, I. Cohen, O. Shochet, A. Czirk, T. Vicsek, Physical Review Letters 75 (1995) 2899.

[15] E. Ben-Jacob, I. Cohen, A. Czirók, T. Vicsek, D.L. Gutnick, Physica A 238 (1997) 181.

[16] M.P. Brenner, L.S. Levitov, E.O. Budrene, Biophysical Journal 74 (1998) 1677.

[17] E.O. Budrene, H.C. Berg, Nature 376 (1995) 49.

[18] Y. Harada, A. Nogushi, A. Kishino, T. Yanagida, Nature (London) 326 (1987) 805.

[19] M. Badoual, F. Jülicher, J. Prost, Proceedings of the National Academy of Sciences of the United States of America 99 (2002) 6696.

[20] C. K. Hemelrijk, H. Kunz, Behavioral Ecology 16 (2005) 178.

[21] D.J. Hoare, I. D. Couzin, J.-G.J. Godin, J. Krause, Animal Behaviour 67 (2004) 155.

[22] T. Vicsek, A. Cziró, E. Ben-Jacob, I. Cohen, O. Shochet, Physical Review Letters 75 (1995) 1226.

[23] A. Czirók, H. E. Stanley, T. Vicsek, J. Physica A 30 (1997) 1375.

[24] T. Iliass, D. Cambui, L. Youssef, Chinese Journal of Physics 54 (2016) 108114.

[25] Buhl, J., Sumpter, D.J.T., Couzin, I.D., Hale, J.J., Despland, E., Miller, E.R., Simpson, S.J., Science 312 (2006) 1402.

[26] Ch. Becco, N. Vandewalle, J. Delcourt, P. Poncin, Physica A 367 (2006) 487.

[27] Szabö, B., Szöllösi., GJ, Gönci, B., Jurányi, Z., Selmeczi, D., and Vicsek, T., Physical Review E 74 (2006) 061908.

[28] Makris N. C., Ratilal P., Jagannathan S., Gong Z., Andrews M., Bertsatos I., Rune Godø O., Nero R. W., Jech J. M., Science 323 (2009) 17341737.

[29] I. Aoki, Bulletin of the Japanese Society of Scientific Fisheries 48 (1982) 1081.

[30] A. Huth, C. Wissel, Journal of Theoretical Biology 156 (1992) 365.

[31] I. D. Couzin, J. Krause, R. James, G. D. Ruxton, N. R. Franks, Journal of Theoretical Biology 218 (2002) 1.

[32] D.S. Cambui, A. Rosas, Physica A 391 (2012) 3908.

[33] D. Cambui, International Journal of Modern Physics B 28 (2014) 1450094.

[34] D.S. Cambui, Chinese Journal of Physics 53 (2015) 100902.

[35] N. Moussa, I. Tarras, M. Mazroui, Y.Boughaleb, International Journal of Modern Physics C 22 (2011) 661.

[36] I. Tarras, N. Moussa, M. Mazroui, Y. Boughaleb, A. Hajjaji, Modern Physics Letters B 27 (2013) 1350028.

[37] Y. Lachtioui, A. Kotri, I. Tarras, K.Saadouni, M.Mazroui, Molecular Crystals and Liquid Crystals 628 (2016) 8698.

[38] T. Iliass, D. Cambui, International Journal of Modern Physics B 30 (2016) 1650002.

[39] I. Tarras, N. Moussa, M. Mazroui, Y. Boughaleb, International Journal of Computer Applications 46 (2012) 21.

[40] G. Baglietto, E.V. Albano, Computer Physics Communications, 180 (2009) 527.

[41] M. Nagy, I. Daruka, T. Vicsek, Physica A 373 (2007) 445454.

[42] D.S. Calovi, U. Lopez, S. Ngo, C. Sire, H. Chaté, G. Theraulaz, New Journal of Physics 16 (2014) 015026.

[43] E.V. Albano, Physical Review Letters 77 (1997) 2129.

[44] G. Grégoire, H. Chaté, Physical Review Letters 92 (2004) 025702.

[45] I. Aoki, Bulletin of the Ocean Research Institute 12 (1980) 1.

[46] K. Binder, D. W. Herrmann, Monte Carlo Simulation in Statistical Physics: An Introduction, 3rd ed. (Springer, Berlin, 1997).

[47] V. Privman, Finite-Size Scaling and Numerical Simulation of Statistical Systems (World Scientifc, Singapore,1990).

[48] D.S. Cambui, A.S. de Arruda and M. Godoy, International Journal of Modern Physics C 23 (2012) 1240015.

[49] I. Tarras, M. Mazroui, N. Moussa, Y. Boughaleb, Modern Physics Letters B 28 (2014) 1450137.